vehicles. The results from the design equations were compared with results from a three-dimensional FEA for both a large and a small leading-edge radius. The results compared quite well for most cases and indicate that the equations can be used for a quick assessment of a preliminary heat-pipe-cooled leading-edge design. If a feasible design is indicated, a more detailed analysis should follow.

Acknowledgment

The author would like to thank the Thermal Structures Branch at NASA Langley Research Center for funding this work under Contract NAS1-96014.

References

[1]Glass, D. E., and Camarda, C. J., "Preliminary Thermal/Structural Analysis of a Carbon-Carbon/Refractory-Metal Heat-Pipe-Cooled Wing Leading Edge," *Thermal Structures and Materials for High Speed Flight*, edited by E. A. Thornton, Vol. 140, Progress in Astronautics and Aeronautics, AIAA, Washington, DC, 1992, pp. 301–322.

[2]Glass, D. E., "Closed Form Equations for the Preliminary Design of a Heat-Pipe-Cooled Leading Edge," NASA CR-1998-208962, Dec. 1998.

[3]Glass, D. E., Camarda, C. J., Merrigan, M. A., and Sena, J. T., "Fabrication and Testing of Mo-Re Heat Pipes Embedded in Carbon/Carbon," *Journal of Spacecraft and Rockets*, Vol. 36, No. 1, 1999, pp. 79–86.

M. Torres
Associate Editor

Effects of Arcing on Insulator Surface Potential in Plasma: Image Observation

Mengu Cho,* Naoki Miyata,† and Masayuki Hikita‡
Kyushu Institute of Technology,
Kitakyushu 804-8550, Japan

Introduction

THE use of high power in future space missions, especially in low Earth orbit (LEO), calls for high-voltage power generation and transmission, typically higher than 100 V. When solar arrays generate electrical power at a high voltage, most of the voltage becomes negative with respect to the plasma due to the low mobility of ions.[1] Arcing is known to occur at the negative part of the solar array. The arcing causes various undesired side effects, such as electromagnetic interference and surface deterioration and sometimes leads to the permanent loss of the spacecraft power, such as the case of the Tempo-2 satellite.[2] Preventing arcing is an important technical task to realize a large space platform in LEO that uses high power of the order of 100 kW or more.

A conventional design of solar arrays has a series of solar cells connected by exposed interconnectors with coverglasses placed on top of the cells. The triple junction is formed by the interconnector (electrical conductor), the coverglass (electrical insulator), and the surrounding plasma. Studies on high-voltage solar arrays (see Ferguson et al.[2] and references therein) revealed that arcing occurs at the triple junction once a strong electric field is applied by the charging of the dielectric material. Thieman et al.[3] observed optical flashes along the edge of the coverglass. Vaughn et al.[4] showed that an arc produced a dense plasma that neutralized the positive surface on the nearby dielectric surface.

Cho et al.[5] proposed that the arc rate is given as the inverse of the charging time. The coverglass surface is charged by positive ions that are attracted by the negative potential of the solar cells. At steady state, the surface potential is nearly equal to the space plasma potential. Then, the insulator surface near the triple junction is charged further by secondary electron emission that is released by the impact of electrons emitted from the interconnector surface via field emission. Once an arc occurs, the arc plasma neutralizes the positive charge near the arc spot, and the charging process restarts.

The purpose of this paper is to present the results of direct observation of the charging and discharging process near the arc spot. We have developed an experimental system, which can measure the in situ two-dimensional surface potential distribution over the dielectric material placed in a plasma environment. The system employs a nonlinear optical crystal, $B_{i12}S_iO_{20}$ (BSO), which exhibits the Pockels effect. Miller[6] measured the surface potential by sweeping an electrostatic probe, which disturbed the plasma environment near the test sample and often caused arcing as the probe moved over the exposed conductor. The observation system used in this paper is an optical method and can measure the charge distribution without disturbing the environment near the test sample.

Experiment

Figure 1 shows a schematic of the experimental system. The pressure in the vacuum chamber (1 m diameter and 1.2 m length) is 8×10^{-2} Pa when the diffusive argon plasma source is operated. The plasma density is 10^{11} m^{-3}, and the electron temperature is 1 eV. The plasma potential with respect to the grounded chamber wall is approximately +10 V. The test sample consists of an indium tin oxide (ITO) electrode (4 × 4 cm), BSO crystal (1 × 1 cm and 1 mm thickness), and polyimide film (25 μm thickness). The test sample is placed on acrylic plate and biased to −1 kV. The BSO

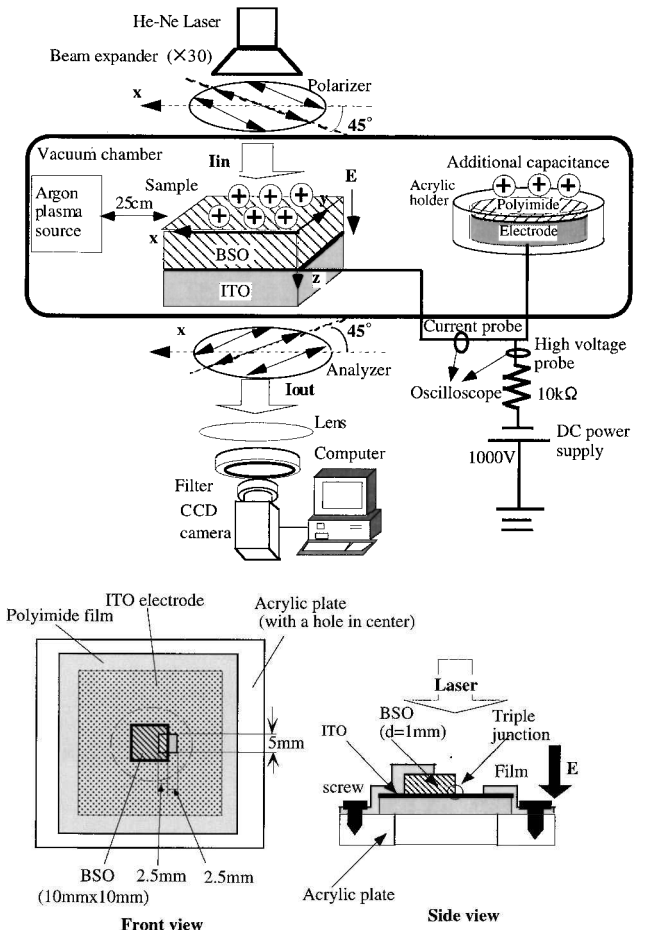

Fig. 1 Schematic of experiment setup.

Received 9 July 1999; revision received 5 October 1999; accepted for publication 9 October 1999.

*Associate Professor, Department of Electrical Engineering. Member AIAA.

†Graduate Student, Department of Electrical Engineering; currently Engineer, Power Division, Shikoku Electric Power Co., Inc., Matsuyama 790-0951, Japan.

‡Professor, Department of Electrical Engineering.

crystal is placed on top of the ITO electrode and mostly covered by the polyimide film with a square opening of 5 × 5 mm. The opening produces the triple junction along the edge of the polyimide film and the BSO crystal. The BSO crystal acts not only as the measurement probe but also as the model of dielectric coverglass of a solar array. The dielectric constant of BSO is approximately 5×10^{-10} F/m. The ITO electrode acts as the model of an interconnector. Inside the chamber we also placed an additional capacitance, 20 nF, made of an electrode insulated by a polyimide film and acrylic holder. This simulates the other part of spacecraft insulator surface, which supplies the arcing current once the arc is initiated.[7]

A helium–neon laser (632-nm wavelength and 20-mW power) is introduced into the chamber through a linear polarizer, whose inclination is 45 deg with respect to the crystal axes. When an electric field is applied in the direction parallel to the laser beam, the Pockels effect elliptically polarizes the incoming linearly polarized light as it passes the BSO crystal. Another linear polarizer is placed in front of a camera, which takes out only the component rotated inside the BSO crystal. The output laser intensity is given by[8]

$$I_{\text{out}} = I_{\text{in}}\left\{1 - \cos\left[(2\pi/\lambda)n_0^3\gamma_{41}Ed\right]\right\} \tag{1}$$

where n_0 is the index of refraction without the external field, $n_0 = 2.56$; γ_{41} is the coefficient to represent the change of the index of refraction due to the external field, $\gamma_{41} = 5 \times 10^{-12}$ m/V; λ is the wavelength; and d is the thickness of the BSO crystal. Before we evacuate the chamber, we apply a known electric field across the BSO crystal to obtain the relationship between the output signal I_{out} and the potential difference across the BSO crystal, Ed. The potential difference calibrated in this way has a typical error of ±100 V.

The image taken by the charge-coupled device camera contains noise caused by stress on the BSO crystal. To remove the noise, we set the polarization planes of the polarizer and the analyzer in the same direction as the crystal axes and take the noise patterns. The Fourier transform of the noise patterns is carried out, and the wavelengths specific to the noise (from 240 to 800 μm) are removed from the measurement. This procedure limits the spatial resolution of the final result to 800 μm.

Results and Discussion

Figure 2 shows the temporal variation of the surface potential distribution on the BSO crystal. In Fig. 2, the triple junction corresponds to the right edge of each image. The surface potential is given by adding the observed potential difference across the BSO crystal, Ed, to the biased potential, V_b (= −1000 V). The potential is referenced to the ground unless stated otherwise. The interlaced video takes 60 fields per second with its exposure time of 33.3 ms. By skipping one field, we can avoid the overlap of 16.7 ms between the adjacent fields. In Fig. 2 we put the exposure time of each field.

Theoretically, an insulator surface on top of a biased electrode placed in a plasma acquires positive charges and acts as a capacitance. The surface charging reaches steady state when the fluxes of electrons and ions to the surface become equal,[1] which is usually attained when the surface has a negative potential comparable to the electron temperature, which is 1 eV for the present case. The surface potential shown in Fig. 2 is near zero before the arcing, which agrees with the theory.

In Fig. 2, we mark the arc site that was identified by an optical flash in the video. The flash was observed in the fields 0 and 1. Therefore, the arc occurred between $t = 0$ and $t = 16.7$ ms, and field 1 contains the images before and after the arc. The arc current monitored by a current probe had a peak value of 12 A and carried the charge of 16 μC. The reading of the high-voltage probe jumped from −1000 to 0 V in 1.5 μs because of the potential drop across the resistance, 10 kΩ, by the arc current. The current increased to 3 A during the first 1.5 μs. Then the current increased to 12 A in another 1.5 μs and decayed to zero in the next 1 μs. During the same experiment, more than 10 arcs with similar events were observed in 30 min.

Once the arc occurs, the ITO potential jumps to near 0 V from −1000 V in 1.5 μs. In such a short timescale, the potential drop across BSO, which is 1000 V before the arc, is still maintained, and its surface potential jumps to +1000 V with respect to the plasma.

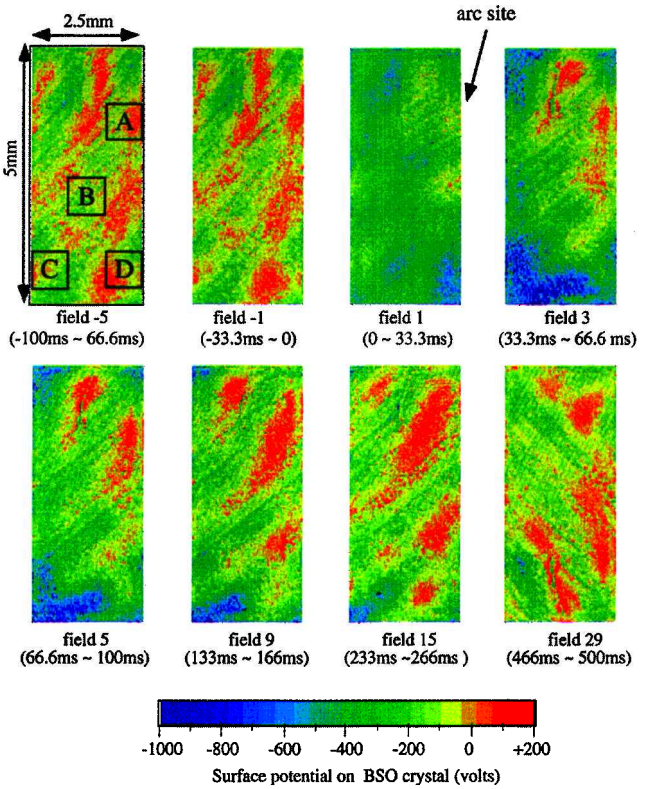

Fig. 2 Temporal variation of surface potential distribution before and after arcing; one field corresponds to 33.3-ms exposure time. Triple junction is at the right edge of each rectangle.

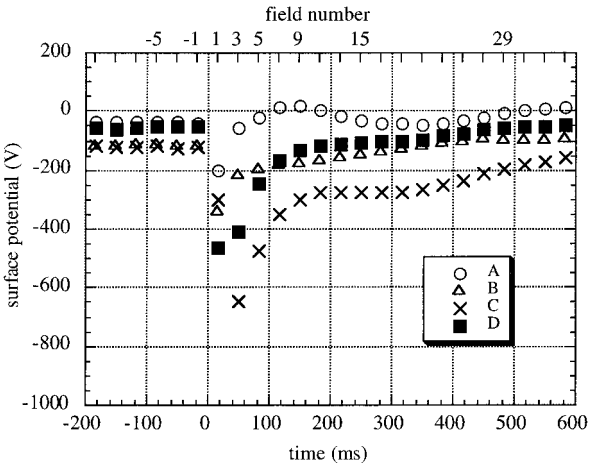

Fig. 3 Temporal variation of surface potential at various points on BSO crystal; time is measured from the time of arcing. Locations A, B, C, and D are shown in Fig. 2.

The insulator surface attracts electrons from the plasma nearby, and the surface charge is rapidly neutralized. This neutralization process also occurs at the additional capacitance and supplies the arc current by forming the current path through the ITO electrode, capacitance, and the plasma, which are isolated from the external power supply. Once the arc current ceases, the ITO potential returns to −1000 V. The BSO surface potential is now less than what it was before the arcing by the amount of neutralized charge divided by the capacitance of BSO. Because the surface potential is now negative, ions are attracted to the surface and recharge it gradually. The process of charge loss from the BSO surface occurs in the timescale of microseconds, which is too fast to observe by the video camera.

In Fig. 3, we plot the temporal variation of the surface potential at various points. The potentials are the averaged values inside the rectangles (800 × 800 μm) shown in Fig. 2. The potential drops

to below −600 V after the arc in curve C. The potential just after the arc should be even lower than this value because field 3 is the image of the recovering process due to ion recharging. The upper right corner of Fig. 2, which is curve A, already shows the recovery in field 3. In field 1, however, even that part shows the decrease of more than 100 V from field −1, indicating the loss of surface charge. The closer the points are to the arc site, the more rapidly the surface potential recovers to the value before the arcing. Whereas curve C takes nearly 1 s to recover to the value before the arc, curve A takes less than 33 ms. The reason why curve A oscillates is unknown.

If all of the charge stored on the BSO surface is discharged in one arc, the BSO potential drops to −1000 V when the arc current is terminated. Then the BSO surface needs to collect 5×10^{-4} C/m^2 to recover from −1000 to 0 V considering its capacitance per unit area, 5×10^{-7} F/m^2. If the ions are attracted by the ion acoustic velocity, 1500 m/s for the present case, the ion density of 2×10^{12} m^{-3} is necessary to provide this charge in 1 s, like curve C in Fig. 3. If it is 33 ms like curve A in Fig. 3, it is 6×10^{13} m^{-3}. These values are higher than the ambient plasma density, 10^{11} m^{-3}. Ambient ions are focused, however, toward the negative surface. Also a very dense plasma is produced at the arc spot when the charge of 16 μC flows in 4 μs. Even after the arc termination, part of the arc plasma remains and diffuses away. If we consider these two points, those ion densities are reasonable, and we can conclude that the recovery of the surface potential is due to charging by ions.

Conclusion

A laboratory experiment was conducted to measure the surface potential of an insulator on top of a negatively biased conductor in a plasma simulating the LEO environment. A nonlinear optical crystal was used to measure the in situ two-dimensional potential distribution over the surface parallel to the underlying electrode via the Pockels effect with a time resolution of 33.3 ms and a spatial resolution of 800 μm. Before an arc, the insulator surface potential is near zero. After the arcing event, the positive surface charge is neutralized within 33 ms, and the surface potential is driven toward the biased electrode voltage. Then the surface is recharged by the plasma nearby and recovers to the condition before the arcing in about 1 s. This process was observed to occur repeatedly. The repetitive process of charging and discharging of insulator surface has been proposed in theories and numerical simulations. The result presented in this Note gives experimental proof of this process.

The surface potential distribution measurement system described has room for improvement. The time resolution can be improved by employing a faster video system. The spatial resolution and quantitative accuracy can be improved by reducing the noise. The key to development of high-voltage devices for space use is how to prevent the charging near the triple junction. The improved observation system will be used to verify various new designs of the devices in laboratory experiments.

Acknowledgment

This study is funded by a part of "Ground Research for Space Utilization" program by the National Space Development Agency and the Japan Space Forum.

References

[1]Hastings, D. E., and Garret, H., *Spacecraft Environmental Interactions*, Cambridge Univ. Press, New York, 1996, Chap. 5.

[2]Ferguson, D. C., Snyder, D. B., Vayner, B. V., and Galofaro J. T., "Array Arcing in Orbit—from LEO to GEO," AIAA Paper 99-0218, Jan. 1999.

[3]Thieman, H., Schunk, R. W., and Bogus, K., "Where Do Negatively Biased Solar Arrays Arc?," *Journal of Spacecraft and Rockets*, Vol. 27, No. 4, 1991, pp. 563–565.

[4]Vaughn, J. A., Carruth, M. R., Katz, I., Mandell, M. J., and Jongeward, G. A., "Electrical Breakdown Currents on Large Spacecraft in Low Earth Orbit," *Journal of Spacecraft and Rockets*, Vol. 31, No.1, 1994, pp. 54–59.

[5]Cho, M., and Hastings, D. E., "Dielectric Charging Processes and Arcing Rates of High Voltage Solar Arrays," *Journal of Spacecraft and Rockets*, Vol. 28, No. 6, 1991, pp. 698–706.

[6]Miller, W. L., "An Investigation of Arc Discharging on Negatively Biased Dielectric-Conductor Samples in a Plasma," *Spacecraft Environmental Interaction Technology—1983*, NASA CP-2336, 1983, pp. 367–377.

[7]Cho, M., Miyata, N., Hikita, M., and Sasaki, S., "Discharge over Spacecraft Insulator Surface in Low Earth Orbit Plasma Environment," *IEEE Transactions on Dielectrics and Electrical Insulation*, Vol. 6, No. 4, 1999, pp. 501–506.

[8]Kawasaki, T., Terashima, T., Yongchang, Z., and Takada, T., "AC Surface Discharge on Dielectric Materials Observed by Advanced Pockels Effect Technique," *Journal of Applied Physics*, Vol. 76, No. 6, 1994, pp. 3724–3729.

A. C. Tribble
Associate Editor